

## THE FORMATION OF PLANETS

STEVEN P. RUDEN

*University of California, Irvine*  
*Department of Physics and Astronomy*  
*Irvine, CA 92697*  
*USA*

### 1. Introduction

Mankind has attempted to understand the origin of the Earth and planets for countless generations. In the past few decades, starting largely from the pioneering work of Safronov in the 1960s, philosophical speculation about their birth has been replaced with detailed analytical and numerical simulations whose goal is to reproduce the observed properties of our own solar system. With the recent groundbreaking discoveries of planets around ordinary stars like our Sun (Mayor & Queloz 1995; Marcy & Butler 1996; Butler & Marcy 1996; see also the review by Marcy in this volume), we now have a reasonable sample of nearby planetary systems that we can use to test and validate theoretical models and from which we can learn new and unexpected features of planet formation. In the upcoming decade the launches of NASA's Space Interferometry Mission (SIM) and ESA's Global Astrometric Interferometer for Astrophysics (GAIA) (and their longer term counterparts Terrestrial Planet Finder [TPF] and Infrared Space Interferometry Mission [IRSI]) will allow us to detect *directly* planets around nearby stars, which will give us an even more complete census of the number and content of planetary systems in the Solar neighborhood. To place this observational data in a proper astrophysical context, we need to understand how planets are born and how they interact with their environment. In this review, I will discuss the dynamics of the growth of solid particles from initially micron-sized dust grains through kilometer-sized planetesimals to their final planetary mass. I will also discuss the formation of the gas-rich giant planets and their tidal interaction with the surrounding nebular disk. The reader interested in further details of the planet formation process

is encouraged to consult the excellent reviews by Lissauer (1993) and by Marcy and Butler (1998).

### 1.1. OVERVIEW: FROM DUST TO PLANETS

The low eccentricities and inclinations of the planets (see Table 1) have long been used as evidence that the Solar System formed from a flattened disk of gas and dust: the *primordial solar nebula*. The recognition that the collapse of magnetized, rotating molecular cloud cores naturally leads to protostellar disks with roughly the right mass and size ( $\sim 100$  AU) is one of the successes of modern star formation theory (for a thorough review see Shu, Adams, & Lizano 1987). The solid content in these disks is comprised of the interstellar grains that survive their passage into the disk (through a surface disk shock) plus nebular volatiles that condense as dust within the disk. In the current “standard model” of planet formation, the rocky cores of all planetary bodies grow from the accumulation of small dust grains; the increase in growth is tremendous – nearly a factor of  $10^{13}$  in size and  $10^{40}$  in mass. In our Solar System, this model is sufficient to explain the formation of the terrestrial planets (Mercury, Venus, Earth, Mars), which have densities comparable to rock (see Table 1) and low-mass gas atmospheres that were most likely outgassed from the rocky material from which they accreted (Brown 1949; Prinn 1982; Pepin 1989). The giant planets (Jupiter, Saturn, Uranus, Neptune), which have much lower mean densities (*cf.* Table 1) and massive gas atmospheres, are also thought to have formed from initially rocky cores<sup>1</sup>. However, once the core mass grows to be larger than a critical value ( $\gtrsim 10M_{\oplus}$ ), rapid accretion of nebular gas transforms them into gas giant planets (Mizuno 1980).

The growth of planet-sized solid bodies conventionally occurs in two loosely defined sequential phases. In the first phase (§3), dust grains, which are uniformly distributed in and strongly coupled to the nebular gas, grow through binary collisions. As they grow larger they settle gravitationally towards the nebular midplane forming a thin layer. Mutual collisions (and possibly gravitational instability of the dust layer) induce further growth in the midplane forming roughly kilometer-sized bodies called *planetesimals*. Planetesimals are, by definition, massive enough to have largely decoupled from the gas and move on nearly circular, Keplerian orbits about the central star. The first phase is believed to be relatively short, occurring on a timescale as little as a few thousand orbital periods (Weidenschilling & Cuzzi 1993). In the second phase, planetesimals continue to grow through inelastic collisions. The essential feature is that collision cross-sections are

<sup>1</sup>Models invoking dynamical gravitational instabilities to form the giant planets (Cameron 1978) have fallen out of favor (see Lin & Papaloizou 1985).

TABLE 1. Properties of Solar System Planets

Planet	Orbital Semimajor Axis (AU)	Mass ( $M_{\oplus}$ )	Mean Density ( $\text{g}/\text{cm}^3$ )	Eccentricity	Inclination (degrees)
Mercury	0.39	0.055	5.4	0.20	7
Venus	0.72	0.82	5.2	0.007	3
Earth ( $M_{\oplus}$ )	1.0	1.0	5.5	0.02	0
Mars	1.5	0.11	4.0	0.09	1
Jupiter	5.2	318	1.3	0.05	1
Saturn	9.6	95.1	0.70	0.06	2
Uranus	19	14.5	1.6	0.05	1
Neptune	30	17.2	1.6	0.009	2

Notes: Pluto is not included because it is more typical of the low-mass outer Solar System Kuiper belt objects.  
 $1M_{\oplus} = 6 \times 10^{27}\text{g} = 3 \times 10^{-6}M_{\odot}$

increased above their geometrical value by the focusing nature of the gravitational interaction between the colliding planetesimals (Safronov 1972). If the relative velocity dispersion among the planetesimals remains sufficiently small, the increase in cross-section is greatest for the most massive planetesimal. This planetesimal will then collide more frequently and gain mass more rapidly than its neighbors, which causes its collision cross-section to increase even further. “Runaway” growth occurs in which the most massive planetesimal accretes all the available solid matter in its local “accretion zone” – the region of the disk over which its gravity can perturb nearby planetesimals into colliding orbits. The runaway process produces a series of rocky protoplanetary bodies that are dynamically and physically isolated from each other and occurs on timescales of  $\sim 10^6$  years (Wetherill & Stewart 1989; Aarseth, Lin, & Palmer 1993; Weidenschilling, *et al.* 1997). After the runaway stalls because all the available nearby solid matter has been accreted, further collisional growth of the protoplanets can occur but only on much longer timescales ( $\sim 10^8$  years) as mutual gravitational perturbations cause orbits to cross and highly inelastic collisions to occur (Wetherill 1980; Chambers, Wetherill, & Boss 1996).

As the planets grow, they find themselves in a nebular environment that changes with time as the gas in the disk is accreted by the central star (Ruden & Lin 1986). Eventually, the disk is cleared of gas via processes such as stellar winds or UV irradiation by the central star (Shu, Johnstone, & Hollenbach 1993). The growth of the terrestrial planets to their cur-

rent masses could have continued long after the dispersal of the gas disk. However, because the more massive atmospheres of the giant planets were accreted from the nebular gas disk, the growth of their rocky cores to the critical mass had to be complete *before* disk dispersal. Observations indicate protostellar disk lifetimes are  $\lesssim 10^7$  years (Strom, *et al.* 1989; Beckwith, *et al.* 1990; Zuckerman, Forveille, & Kastner 1995; see also the review by Beckwith in this volume), placing an important time constraint on the planet formation process. Current models have difficulty forming the giant planet cores on this timescale unless the mass of the solar nebula is significantly larger than the minimum-mass solar nebula.

The giant planets are massive enough that gravitational tidal interactions between the planet and the surrounding disk can create annular gaps largely devoid of gas at the orbit of the planet. This mechanism of *tidal truncation* (Lin & Papaloizou 1993) has been invoked to explain why the giant planets stop their rapid gas accretion and thus attain their final masses (§5.2). The tidal interaction also causes the orbital semimajor axes of the planets to decrease in time. This *orbital migration* of the giant planets is a serious problem that will be discussed in more detail in §5.3.

## 1.2. FUTURE RESEARCH QUESTIONS

Throughout this review I will list a selection of the major unsolved questions in planet formation theory. I hope these questions will provoke and encourage the reader to consider devoting some thought to their solution.

- When does the planet building epoch begin?
  - Is it a continuous process beginning from the initial formation of the disk?
  - Does planet formation require some critical conditions (such as a sufficiently cool or quiescent nebula) before it begins?
- How does planet formation modify the disk environment and its evolution?
  - Are there unambiguous observable signatures such as holes or gaps?
- What outcomes are likely?
  - A diverse planetary system like our own?
  - Giant planets close to the central star as in 51 Pegasus?
  - Rubble disks like  $\beta$  Pictoris?

## 2. Structure and Evolution of Disks

Protoplanetary disks are just one example of an accretion disk – a geometrically thin disk of gas (and dust) revolving around a central mass point (Pringle 1981; Lin & Papaloizou 1985; and the review chapter by Kenyon in this volume). We can understand their basic properties by examining the force balance equations assuming the gas is in orbit around a central protostar with mass  $M_*$ . Adopting cylindrical coordinates  $(r, \phi, z)$  and assuming axisymmetry, the disk is in vertical hydrostatic equilibrium where the vertical pressure force balances the vertical component of the central star's gravity

$$\frac{1}{\rho} \frac{\partial P}{\partial z} = -\frac{GM_*}{r^2} \left( \frac{z}{r} \right) \equiv -\Omega^2 z, \quad (1)$$

where  $P$  and  $\rho$  are the gas pressure and density, and where we have defined the Keplerian rotation rate

$$\Omega = \sqrt{\frac{GM_*}{r^3}}. \quad (2)$$

We can scale equation (1) to find an expression for the vertical height of the nebula,  $H$ ,

$$H = \frac{c}{\Omega}, \quad (3)$$

where the nebular sound speed  $c$  is defined by the relation  $P = \rho c^2$ . We say the disk is geometrically thin if  $H \ll r$ , which from equation (3) is equivalent to the disk being dynamically cold,  $c \ll \Omega r$ , *i.e.*, the nebular sound speed is much less than the orbital Kepler speed. Because disks are thin, it is convenient to use vertically averaged quantities such as the surface density,  $\Sigma$ :

$$\Sigma = \int_{-\infty}^{+\infty} \rho dz \approx 2\rho H = 2\frac{\rho c}{\Omega}, \quad (4)$$

where we interpret  $\rho$  in the last two terms on the right side of the equation as the value of the density at the midplane of the nebula.

Force balance in the radial direction is given by

$$\frac{v^2}{r} = \frac{GM_*}{r^2} + \frac{1}{\rho} \frac{\partial P}{\partial r}, \quad (5)$$

where  $v$  is the orbital speed of the gas. For thin, cold disks, the radial pressure gradient is smaller than the stellar gravitational force by  $\sim (H/r)^2 \ll 1$  (as may be verified by scaling eq. [5] and using eq. [3]) and is typically neglected in most accretion disk applications. In this case, equation (5) shows the gas rotates in centrifugal balance at the Keplerian orbital speed,  $v = \Omega r$ .

In most disks, the pressure is largest near the star and decreases outward so that the radial pressure term in equation (5) is negative. This means the pressure of the gas partially supports the disk against gravity, and the disk gas rotates at a slightly *sub-Keplerian* speed  $v = \Omega r - \Delta v$  with  $\Delta v > 0$ . If we substitute this expression for  $v$  into equation (5), we find

$$\Delta v = \frac{1}{2} \left| \frac{\partial \ln P}{\partial \ln r} \right| \frac{c^2}{\Omega r} \approx \frac{c^2}{\Omega r} = \left( \frac{H}{r} \right) c \ll c, \quad (6)$$

where we have used equation (3) in the last terms on the right. The departure from Keplerian motion is indeed very small being much less than the sound speed which is itself much less than the Keplerian rotation speed. We shall see in §3.1 that this small departure from exact Keplerian rotation plays a critical role in the motion of solids in protoplanetary disks.

In two seminal papers, Lynden-Bell & Pringle (1974) and Shakura & Sunyaev (1973) demonstrated that the evolutionary behavior of accretion disks is governed by the *outward* transport of angular momentum, which allows mass to flow *inward* to be accreted by the central object. The precise mechanisms that cause the transport in *any* astrophysical disk are still far from certain. Numerous suggestions have been made in the case of protostellar disks (see the review by Adams & Lin 1993): gravitational instabilities (Lin & Pringle 1987; Shu, Tremaine, Adams, & Ruden 1990), magnetic instabilities (Stepinski & Levy 1990; Balbus & Hawley 1991), thermal convective instabilities (Lin & Papaloizou 1980; Ruden & Lin 1986), stellar or disk winds (Hartmann & MacGregor 1982; Wardle & Königl 1993) and fluid dynamical shear instabilities (Dubrulle 1993). In most applications, the details of the physical cause of the transport are ignored and angular momentum is assumed to be transported by some form of localized fluid dynamical turbulence that creates an eddy viscosity in the gas. The disk evolution is governed by the magnitude of the turbulent viscosity,  $\nu$ , which is the product of the turbulent eddy size,  $\ell_t$ , and velocity,  $v_t$ . The eddies are assumed to move subsonically and to have sizes smaller than the vertical height of the disk, which leads to the well-known parameterization of the viscosity as (Shakura & Sunyaev 1973)

$$\nu \sim v_t \cdot \ell_t \equiv \alpha c H, \quad (7)$$

where  $\alpha \lesssim 1$  is a dimensionless parameter. Under the action of viscous stress, an initial surface density distribution evolves diffusively by spreading outward while transferring mass inward to be accreted by the central protostar. The viscous evolutionary timescale is

$$t_{\text{vis}} \approx \frac{r^2}{\nu} \approx \frac{1}{\Omega} \frac{1}{\alpha} \left( \frac{r}{H} \right)^2, \quad (8)$$

$$\approx 10^7 \left( \frac{10^{-2}}{\alpha} \right) \left( \frac{r/H}{25} \right)^2 \left( \frac{r}{100\text{AU}} \right)^{3/2} \text{ years.}$$

The solids in protoplanetary disks find themselves in a continuously changing nebular environment in which temperature, density, pressure, and turbulent velocity typically decrease with time (after transients from the initial distribution of matter decay; see Fig. 1). Detailed calculations using reasonable values for the eddy viscosity ( $\alpha \approx 10^{-2}$ ) yield evolutionary times of order  $10^6 - 10^7$  years (Ruden & Lin 1986; Ruden & Pollack 1991), which are in agreement with the observational disk lifetimes cited above.

### 2.1. THE MINIMUM-MASS SOLAR NEBULA (MMSN)

The Solar System was formed from the collapse of a molecular cloud having solar element abundances, yet the present day planets are clearly of non-solar composition. We can ask the important cosmogonical question, “How much *solar composition* gas is required to make the planets?” The mass and inferred spatial distribution of this gas are known as the *Minimum-Mass Solar Nebula* (hereafter, MMSN). The answer to this question has been given by several authors (Weidenschilling 1977a; Hayashi 1981) who take the present amount of condensed solid matter in the Solar System and augment it to solar composition to determine the minimum mass. The radial surface density distribution of this mass is deduced by smearing out the augmented mass of a planet over an area defined by its nearest neighbors.<sup>2</sup>

A key ingredient in the analysis is the dust-to-gas ratio,  $\zeta$ , which measures the mass fraction of dust (*i.e.*, high- $Z$  elements) in a solar composition gas. In cool regions of the nebula with temperatures below about 170 K, both rocky and icy material (such as water, methane and ammonia) can condense from the gas giving the dust-to-gas ratio a value  $\zeta \approx 1/60$  (Hayashi 1981). In warmer regions (above 170 K but below about 1500 K where much of the dust evaporates) only the more refractory (high condensation temperature) solids survive and the dust-to-gas ratio drops by a factor of four to  $\zeta \approx 1/240$  (Hayashi 1981). To find a rough value for the mass in the MMSN we must estimate the present amount of solids in the planets. This comes almost entirely from the high- $Z$  material inside the giant planets, which is estimated to range from 40 - 80  $M_{\oplus}$  (Hubbard & Marley 1989; Chabrier, *et al.* 1992) compared to only 2  $M_{\oplus}$  in the terrestrial planets. Adopting a value of 60  $M_{\oplus}$  for the present mass of condensed solids and an average dust-gas-ratio of 1/100 gives a rough estimate of 6000  $M_{\oplus} \sim 0.02M_{\odot}$  for the mass of solar composition gas needed to make the

<sup>2</sup>An important assumption is that the planets formed at their present locations.

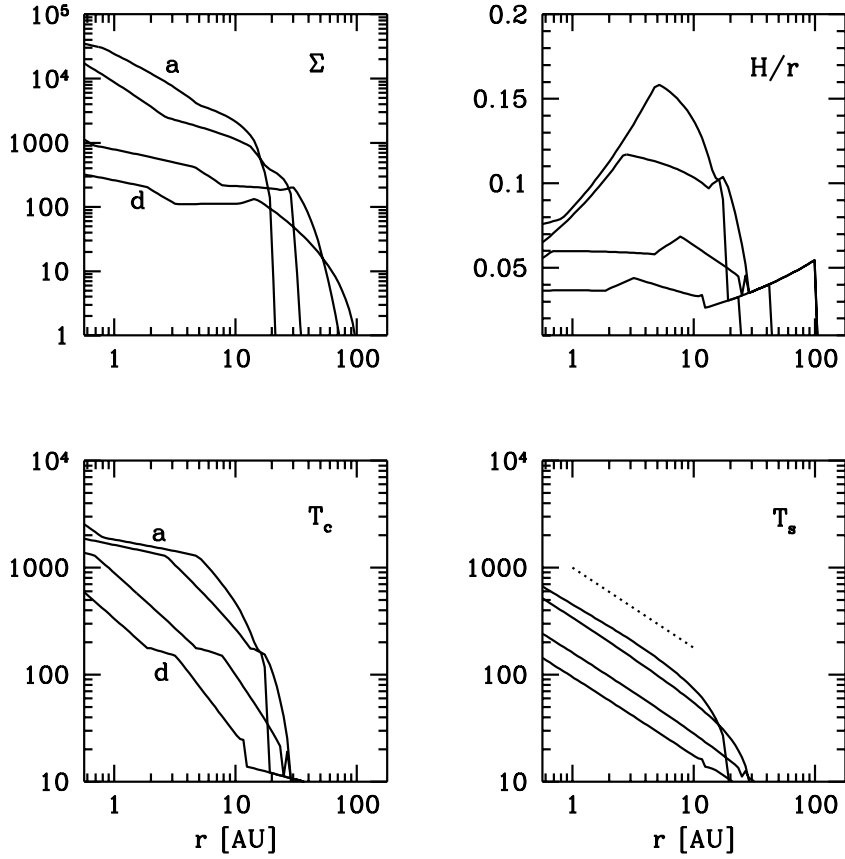


*Figure 1.* Models for the evolution of the primordial solar nebula. Surface density,  $\Sigma$ , aspect ratio,  $H/r$ , central (midplane) temperature,  $T_c$ , and surface (effective) temperature,  $T_s$ , are plotted versus distance from the sun (in AU) for the times a)  $10^3$ , b)  $10^4$ , c)  $10^5$ , d)  $10^6$  years. Note the diffusive spreading of the nebula from less than 10 AU to 100 AU, and the cooling of the nebula with time. The disk always remains geometrically thin ( $H/r \ll 1$ ), and at late times  $H/r \approx 1/25$ . The surface temperature falls off as  $r^{-3/4}$  (marked as the dotted line) away from the outer disk edge. The viscous  $\alpha$  parameter is  $10^{-2}$  in these calculations adapted from Ruden & Lin (1986).

planets.<sup>3</sup> A more detailed calculation of the MMSN by Hayashi (1981) is illustrated in Figure 2. Disk masses derived from millimeter observations of nearby star forming regions are found to range from  $0.005 - 0.2 M_\odot$  (Beck-

<sup>3</sup>Adding the mass of solar composition gas already present in all the planetary atmospheres ( $\lesssim 400M_\oplus$ ) is only a small correction.

with & Sargent 1996; also see the review by Beckwith in this volume), comparable to the MMSN.

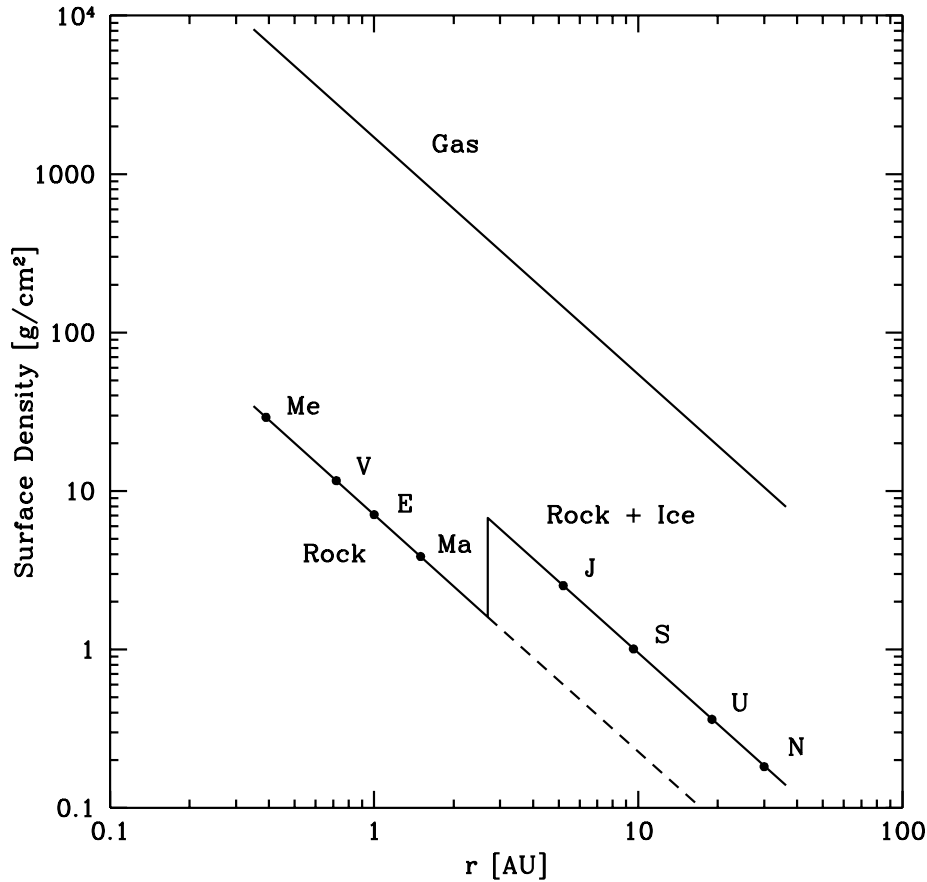


*Figure 2.* Surface density distribution in the Minimum-Mass Solar Nebula (MMSN) adapted from Hayashi (1981). The planets are denoted by Me, V, E, Ma, J, S, U, N. Outside 2.7 AU the temperature is deduced to be cool enough for ices to condense, which causes the surface density of solids to jump by a factor of four. The gas distribution shows no discontinuity, and the surface density of both gas and solids falls off as  $r^{-3/2}$ . The total mass between 0.35 AU and 36 AU is  $0.013 M_{\odot}$ .

The MMSN, while playing a useful role as a conceptual guide, is perhaps becoming overused as a quantitative “reference” standard in model calculations of the planet formation epoch. The planets formed in an *evolving* disk whose properties (such as the position where ices condense) changed with time; the static  $r^{-3/2}$  surface density distribution presented by the

MMSN may not only be quantitatively wrong, but misleading is well. If it does accurately describes any part of the evolution of the solar nebula, it is probably the *final* stages when planet formation is complete rather than the *initial* stages when planet formation began. Furthermore, as we will see in §5.3, it is now thought that orbital evolution of the giant planet semimajor axes may have occurred, which would modify any current reconstruction of the MMSN surface density distribution from that depicted in Figure 2.

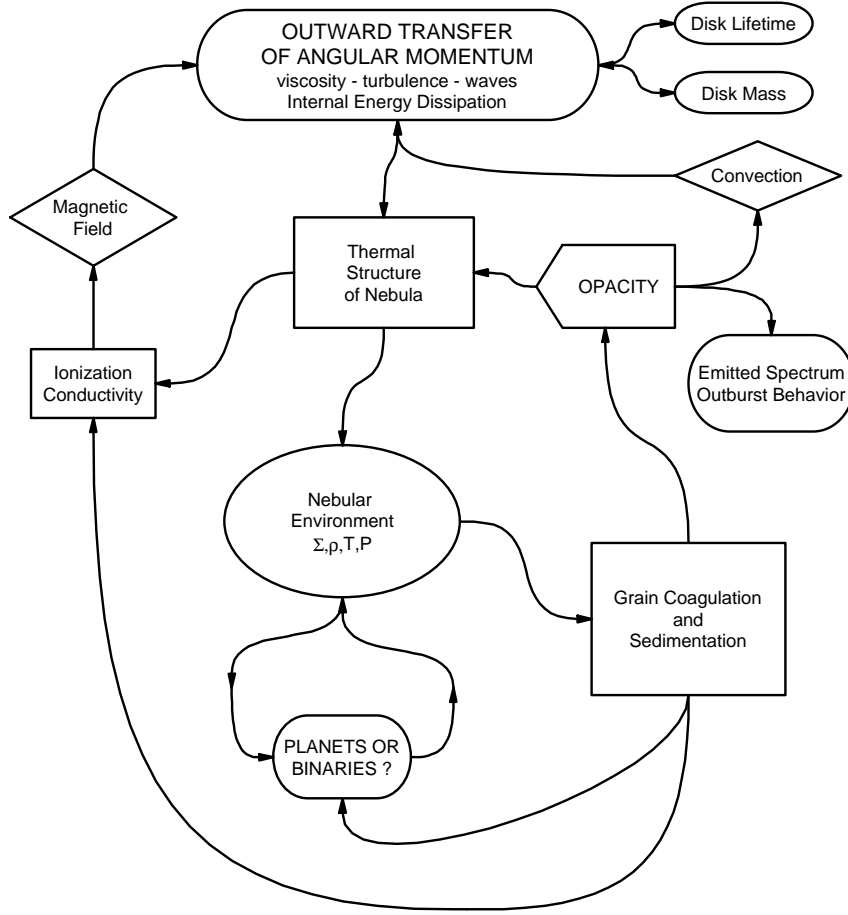
## 2.2. NONLINEAR NATURE OF DISK PHYSICS

It is obvious there is a very complicated interrelationship among all the physical processes that can occur in protoplanetary disks. Figure 3 is an intentionally complicated schematic diagram indicating some of the predominant physical processes, their dependencies and their feedbacks. Although there are many models by many different research groups addressing the key underlying physics in any one of the boxes in Figure 3, successful integration of the different processes together into a coherent whole has been elusive. There are several reasons for this: the inherent complexity of the physics involved, the lack of experimental guidance as to the magnitude of important physical parameters, the inability of current observational techniques to probe the relevant scales (which occur at angular resolutions of  $\sim 10^{-2}$  arcseconds in the nearest star forming complexes) and the nonlinear interplay among the processes themselves. For these reasons, we are far from having a theory that can predict the type of planetary system formed from a given nebular environment. Furthermore, researchers have typically focused their modeling on explaining the properties of our own Solar System, perhaps rejecting scenarios that, although inadequate for our own system, might be good representations of the physics in other protoplanetary disks. As is often the case, more complete observational data will enable modelers to explain the diversity of planetary systems found in nature.

## 3. From Grains to Planetesimals

### 3.1. PARTICLE-GAS DYNAMICS

The motion of solid particles in protoplanetary disks is affected by the drag they experience as they move through the gaseous background of the nebula (Whipple 1972; Adachi, Hayashi, & Nakagawa 1976; Weidenschilling 1977b). We will consider the solids as spheres of radius  $a$  having internal mass density  $\delta$  (to be distinguished from the ambient gas density  $\rho$ ) and mass  $m = 4\pi\delta a^3/3$ . The form of the gas drag force,  $\mathbf{F}_D$ , depends on the size of the particle, its speed through the gas, and local gas properties. The Epstein drag law, which is appropriate for particles with sizes smaller



**RELATIONSHIPS AND DEPENDENCIES  
AMONG PROTOPLANETARY DISK PROCESSES**

Figure 3. Schematic diagram showing the relationships and feedbacks among nebular processes, many of which are only poorly understood. Small modifications to the underlying physics for any one process may have profound effects on the ultimate evolutionary outcome of the star/disk system.

than the mean free path in the gas, is

$$\mathbf{F}_D = -\frac{4}{3} \pi a^2 \rho c \mathbf{v}, \quad (9)$$

where  $c$  is the gas sound speed and  $\mathbf{v}$  is the velocity of the particle relative to the gas. In most regions of the solar nebula, this law is valid for particles with sizes smaller than a few centimeters (see the references above for a

complete list of the different drag law regimes); for simplicity of presentation in this review, I will adopt equation (9) as the principal drag formula. The *stopping time* for a particle is defined to be the time needed for drag to dissipate its momentum,  $t_s \equiv mv/F_D$ . Substituting equation (9) into this definition and eliminating the volume gas density in favor of the surface density from (4), we find the relation

$$\Omega t_s = \frac{\delta a}{\Sigma}. \quad (10)$$

The dimensionless quantity  $\Omega t_s$  is the ratio of the particle stopping time to the local orbital time in the disk and is a key determinant of the dynamical behavior of the particle. In the limit  $\Omega t_s \ll 1$ , the particle, considered “small”, is very strongly coupled to the gas. Drag will force it to move at the local gas velocity, which we saw in §2 to be sub-Keplerian. In the opposite limit,  $\Omega t_s \gg 1$ , the particle, considered “large”, is only weakly perturbed by gas drag and orbits at the Keplerian speed.

Let us consider the dynamics in more detail. At each radius, gas drag forces small particles to orbit at the local gas speed, which is smaller than Keplerian. The net effective gravity (stellar plus centrifugal) acting on the particle points toward the central star, and the particle drifts inward at the terminal speed. This radial velocity is easily shown to be

$$v_r = -2 \Omega t_s \Delta v, \quad (\Omega t_s \ll 1) \quad (11)$$

where  $\Delta v$  is the difference between the Kepler and gas speeds defined in equation (6). Large particles move at the Kepler velocity and experience a headwind as they move through the more slowly moving gas. The gas drag torque causes the orbit of the particle to decay with radial velocity

$$v_r = -\frac{2\Delta v}{\Omega t_s}. \quad (\Omega t_s \gg 1) \quad (12)$$

Detailed calculations by Weidenschilling (1977b; see Fig. 4) verify these limiting behaviors and show that the maximum inward drift speed is  $\approx \Delta v$  and is achieved by particles with sizes that satisfy  $\Omega t_s \approx 1$ . There are several points to note about this inward drift. First, it is size dependent leading to differential speeds among particles with different radius, which can enhance the rate of collisions. Also, the relative speed between bodies entrained in the flow can easily exceed their escape velocities (see Fig. 4). Second, the affect is largest for particles having radii for which  $\Omega t_s \approx 1$ . Using equation (10), we find that the size of these particles is  $a \approx \Sigma/\delta$ , which is of order 1 m at the position of the Earth. Third, although the magnitude of the drift speed is highly subsonic, particles satisfying  $\Omega t_s \sim 1$  decay into

the central star in a time very much less than the evolutionary time of the disk. The drift time for these particles is  $t_{\text{drift}} = r/v_r = \Omega^{-1} (r/H)^2 \approx \alpha t_{\text{vis}} \approx 100(r/\text{AU})^{3/2}$  years. Of course such particles are likely to collide with other solids on their way in and through shattering or growth move to size regimes with smaller drift rates. Nonetheless, gas drag-induced decay is a potentially large sink for the solid component of the disk.

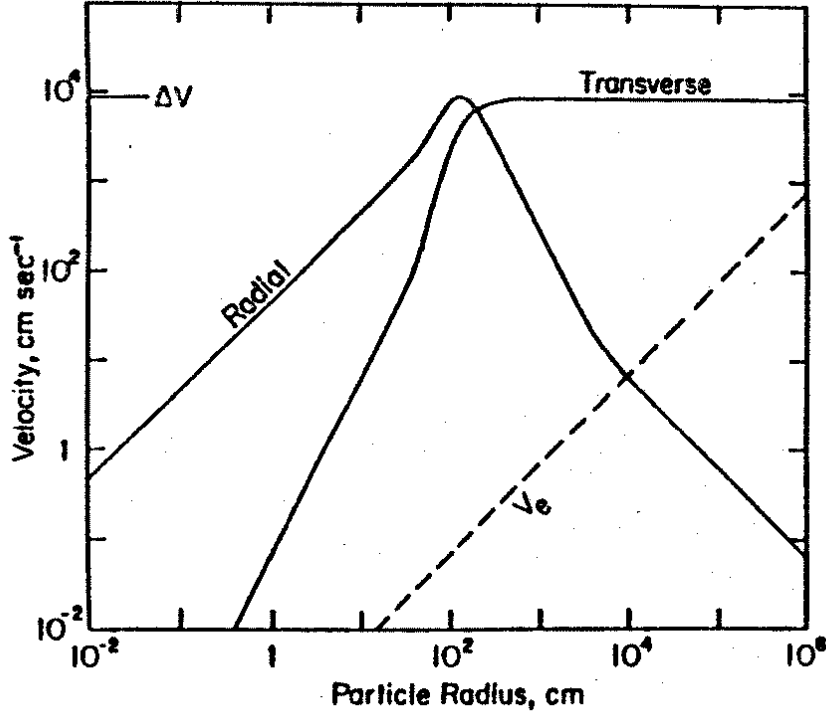


*Figure 4.* Radial and transverse velocity components, relative to the gas, as a function of particle radius. The difference between the Kepler speed and the gas speed is labeled  $\Delta V$ . Small particles have transverse speeds equal to the gas speed, while large particles move at the Kepler speed, *i.e.*, have transverse speeds relative to the gas of  $\Delta V$ . The maximum inward drift speed is  $\approx \Delta V$  and is achieved by particles with  $\Omega t_s \approx 1$ . The changes in slope are transitions between drag regimes, and  $V_e$  is the escape speed from the particle. From Weidenschilling (1977b).

### 3.2. MIDPLANE SETTLING AND GROWTH

As discussed earlier, the formation of solid bodies in the midplane of the nebula begins with agglomeration and sedimentation of smaller grains initially suspended throughout the nebula. Small particles settle in the verti-

cal gravitational field ( $g_z = (z/r)GM_*/r^2 = \Omega^2 z$ ) at the terminal velocity. Using the Epstein law (9), the settling speed and the time to reach the midplane are ( $\Omega t_s \ll 1$ )

$$v_z = -(\Omega t_s) \Omega z, \quad (13)$$

$$t_{\text{settle}} = \frac{z}{|v_z|} = \frac{1}{\Omega} \left( \frac{1}{\Omega t_s} \right) = \frac{1}{\Omega} \left( \frac{\Sigma}{\delta a} \right). \quad (14)$$

The last equation shows that the settling time is always much longer than the rotation period for small grains ( $\Omega t_s \ll 1$ ) and that small grains settle more slowly than larger grains ( $t_{\text{settle}} \propto 1/a$ ). For typical solar nebula conditions the settling time for micron-sized grains is about  $10^6$  years, comparable to the lifetimes of protoplanetary disks. Without collisions to increase grain size (leading to more rapid settling), small grains, which are the dominant contributor to the opacity, will remain suspended in the disk, which will remain optically thick.

Safronov (1972) was one of the first to realize that collisions not only make particles grow but also rapidly decrease the settling time. Equations (13) and (10) show that the settling speed is proportional to the size of the particle. Larger grains will sink towards the midplane faster and will sweep up smaller grains in their path. This causes them to grow larger and to sink even more rapidly. In this manner, the dust component of the disk will therefore “rainout” and form a thin layer of much larger bodies in the midplane of the nebula. We can estimate the size of these bodies by using mass conservation. The total surface density of solids in the disk is  $\zeta \Sigma$ , where  $\zeta$  is the dust-to-gas ratio introduced above. A body that reaches the midplane with final radius  $a$  will have swept up a column of dust having a mass  $p_s \cdot \zeta \Sigma \cdot \pi (a/2)^2$ , where we have taken its average radius on the descent to be  $a/2$  and have introduced the probability of sticking in a collision,  $p_s$ . Equating this to its mass  $m = 4\pi \delta a^3/3$  yields a size

$$a = \frac{3 p_s \zeta \Sigma}{16 \delta}, \quad (15)$$

which is about 1 cm at the Earth in the primordial solar nebula (for  $p_s = 1$ ). The time for solids to sediment to the midplane can be estimated by inserting this value for  $a$  into equation (14); more accurate integrations yield (Nakagawa & Hayashi 1981)

$$t_{\text{sediment}} \approx \frac{100}{\Omega} \frac{1}{p_s \zeta}, \quad (16)$$

which is only a few thousand orbital periods at any point in the disk (again for  $p_s = 1$ ).

There have been several detailed numerical simulations of the collisional growth and sedimentation of dust in the solar nebula (Weidenschilling 1984; Nakagawa, Nakazawa, & Hayashi 1981; Mizuno 1989; Weidenschilling & Cuzzi 1993). A major difficulty with simulating particle growth is our inadequate knowledge of the physical inputs. The sticking probability is a complicated and currently only poorly understood function that depends on the impact velocity and the size, shape and internal strength of the impactors, but it is usually simply taken to be unity for all collisions in the simulation. Realistic nebular particles may have low internal strengths and may shatter in high speed impacts. Some experimental work has been performed on this important issue. Blum & Münch (1993) did not find *any* sticking in collisions between millimeter-sized dust aggregates at speeds  $\lesssim 1$  m/s and found fragmentation at speeds above this. More recently, this group (Wurm & Blum 1998) has investigated lower speed ( $\lesssim 1$  cm/s) collisions between small, porous, fractal grains with sizes  $\sim 10 \mu\text{m}$  and found perfect sticking ( $p_s = 1$ ). In the outer, cooler regions of the nebula volatile ices can form frosts on particle surfaces, which may enhance the sticking probability (Bridges, *et al.* 1996; Supulver, *et al.* 1997).

Turbulence in the gas can have profound affects on the evolutionary simulation. A given sized particle will respond to the fluctuating turbulent velocity field according to whether its stopping time is longer or shorter than the local eddy turnover time. Stirring by turbulence can inhibit sedimentation of particles that have sizes small enough that they are strongly coupled to and co-move with the turbulent eddies. The turbulent velocity field can also greatly increase the relative velocity between particles with different sizes (Markiewicz, Mizuno, & Völk 1991), which can increase the collision rate but also lead to collisions where the bodies shatter (Weidenschilling 1984). Given our poor understanding of turbulence in protoplanetary disks, its effects on grain growth (and vice versa) and grain sedimentation are presently far from clear. Even with these uncertainties and although the individual details vary, the different numerical simulations nonetheless yield midplane particle sizes and sedimentation timescales that are not too dissimilar from the simple estimates above (eqs. [15] & [16]).

### 3.2.1. Radial Distribution of Solids in Protoplanetary Disks

The sedimentation of dust grains produces a thin layer of solids in the nebular midplane. The surface density of this distribution is often taken to be just the gas-to-dust ratio times the local gas surface density,  $\zeta\Sigma$ . To test whether this is a valid approximation and to see whether the solid surface density distribution of the MMSN is reproduced, I have calculated simplified models of the midplane accumulation of solids using the nebular evolutionary models of Ruden & Pollack (1991). The models follow track

the condensed and vapor phases of refractory rocky and volatile icy matter, with ices condensing only in nebular regions with temperatures below 170 K. Early in the evolution, the nebula is too hot for ices to condense anywhere, although rocky matter can condense everywhere outside about 0.1 AU. As the nebula evolves and cools, the radius where ices can condense, *i.e.*, the  $T = 170$  K boundary, moves inward and icy solids sediment. The treatment of grain growth and sedimentation is phenomenologically modeled by allowing the condensed solids to rainout on a timescale given by  $\tau_0/\zeta\Omega$  (*c.f.* eq. [16]), where  $\tau_0$  is an adjustable constant. This model is nonlinear because as the solids sediment to the midplane, the dust-to-gas ratio  $\zeta$  decreases, and the sedimentation time lengthens. Figure 5 shows the results of two evolutionary scenarios: the first with rapid sedimentation,  $\tau_0 = 600$ , and the second with much slower sedimentation,  $\tau_0 = 6 \times 10^4$ . Both models started from the same initial conditions. Significantly more solids are deposited in the midplane in the rapid scenario, but at the time shown in the plot ( $10^5$  years) the nebula is warm enough that ices only condense outside 6 AU. The results of the slow scenario give a surface density distribution comparable to the MMSN after  $\sim 10^6$  years, but with a more shallow slope (and more solid matter) in the outer cool regions.

It seems clear from these idealized models that very different distributions of midplane solid matter are possible, from the same initial mass reservoir, if the sedimentation physics (primarily the average sticking probability) is different. The solid distributions shown in Figure 5 do *not* bear a simple constant multiplicative relationship ( $\zeta\Sigma$ ) to the instantaneous gas surface density distribution. The reason for this is the solids at any given radius were deposited over time and reflect accumulation from different nebular conditions, with primarily rocky material sedimenting early on when the temperature was high followed by icy sedimentation when the nebula was cooler. Note also that the locus at which ice can condense is different in the two models; in general, the midplane distance at which  $T = 170$  K (the ice condensation front) is a function of time.

### 3.3. PLANETESIMAL FORMATION

Planetesimals are bodies large enough to move on Keplerian orbits largely unaffected by gas drag forces over the age of the disk. For typical nebular conditions, bodies larger than about 1 km satisfy this constraint. A key unanswered question is how the smaller sized bodies ( $\sim 1$  cm; eq. [15]) produced in the sedimentation process assemble into planetesimals. The most elegant and efficient mechanism proposed is that the thin layer of solids produced by sedimentation becomes gravitationally unstable and rapidly forms fragments that collapse to produce planetesimals (Goldreich & Ward 1973).

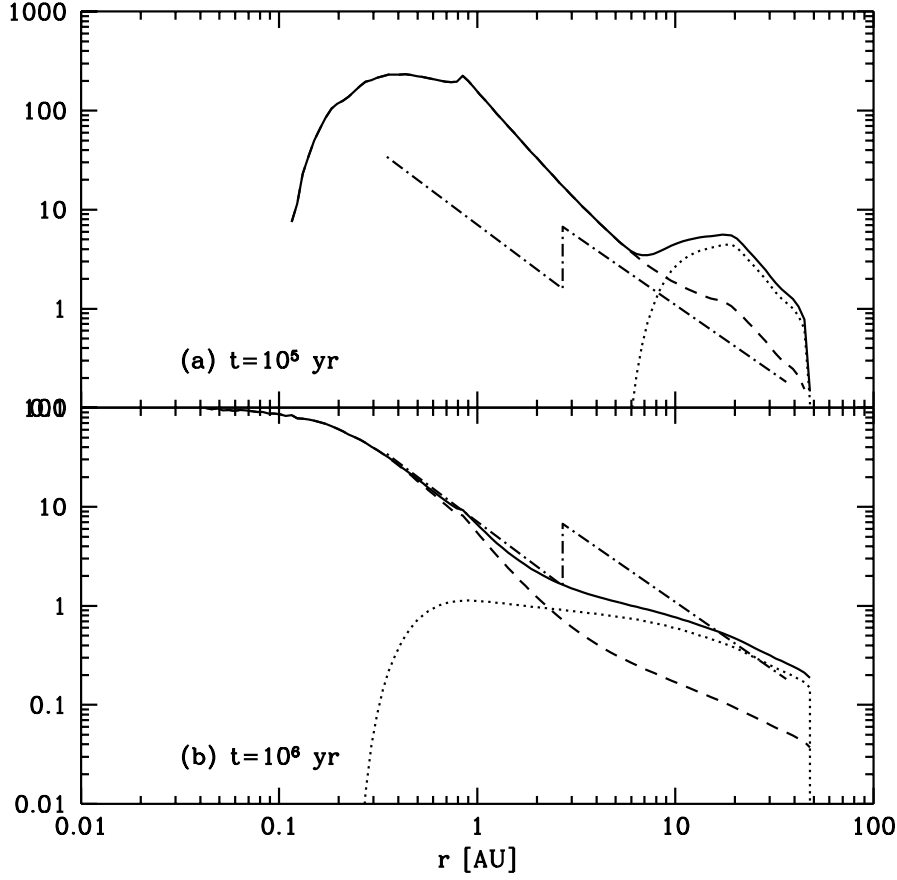


*Figure 5.* Radial distribution of solids in a model of grain growth and sedimentation (Ruden 1998). Surface density (in  $\text{g}/\text{cm}^2$ ) is plotted versus distance in AU. The surface densities of icy (dotted), rocky (dashed), and rock + ice (solid) matter are plotted. The MMSN surface density distribution is shown for comparison (dot-dashed). Panel (a) [(b)] is for the rapid [slow] accumulation scenario, with the evolution times indicated. Note the difference in vertical scale between the panels. See text for further details.

They showed the critical fragmentation lengthscale,  $\lambda_c$ , is

$$\lambda_c \approx 4\pi r \left( \frac{\pi \zeta \Sigma r^2}{M_*} \right), \quad (17)$$

and the typical fragment mass,  $M_{\text{GW}}$  is

$$M_{\text{GW}} = \zeta \Sigma \lambda_c^2 = 16\pi M_* \left( \frac{\pi \zeta \Sigma r^2}{M_*} \right)^3. \quad (18)$$

In these equations, it is the surface density of *solids*,  $\zeta\Sigma$ , that is important, and the ratio in parenthesis is roughly the mass of the solid disk to the protostellar mass. Using nebular parameters from the MMSN, Goldreich & Ward (1973) showed that kilometer-sized bodies can be produced by this gravitational collapse process in a few thousand years.

The Goldreich-Ward instability occurs only in very quiescent dust disks. If the random velocities of the particles composing the dust disk are too large (or equivalently if the dust layer is too thick)<sup>4</sup> then the instability is quenched. The critical random speed is  $\pi G\zeta\Sigma/\Omega$ , which is only about 10 cm/s. In the thin dust disk the solids rotate at nearly the Keplerian velocity while the gas above the layer rotates at a sub-Keplerian rate (eq. [6]). It is thought that turbulence generated by this shear layer will stir up the random velocity in the dust disk and prevent the Goldreich-Ward instability (Weidenschilling & Cuzzi 1993). Detailed hydrodynamical models of the particle-gas interaction have been made by Cuzzi, Dobrovolskis, & Champney (1993) who find that it is unlikely the dust layer can achieve such low random speeds.

If the Goldreich-Ward mechanism does not proceed in protostellar disks, then it is likely that planetesimals are produced in the thin dust layer by inelastic binary collisions. Recall that gas drag causes radially inward flow of solid particles (eqs. [11] & [12]). In the dense particle layer, solids dominate the local density and the drift speed is reduced (Cuzzi, Dobrovolskis, & Champney 1993). Since larger particles have lower drift speeds (eq. [12]), Cuzzi, Dobrovolskis, & Champney (1993) have argued that planetesimals can grow in this layer as the smaller solids drift past them and are collisionally accreted. They estimate that growth to 100 km sizes can be achieved in  $\lesssim 10^6$  years.

#### 3.4. PROSPECTS FOR OBSERVING THE EARLY PLANET FORMATION EPOCH

It would be satisfying if theoretical models gave an unambiguous prediction for the observational signature of grain growth in young protoplanetary disks, for example, the existence of a “hole” in the infrared spectrum (such as the one inferred observationally in HR 4796 by Koerner, *et al.* 1998). Unfortunately, this is presently not the case. In order to “see” forming planets or other structures in the midplane of the disk, the optical depth to the nebular midplane must be small. The disk optical depth is equal to the gas surface mass density times the opacity. The midplane regions can remain cloaked to the eyes of observers if *either* is sufficiently large.

<sup>4</sup>The factor in parentheses in equations (17) & (18) is the maximum value of the aspect ratio,  $H/r$ , the layer can have to be gravitationally unstable.

The primary contributors to the opacity are small grains, but its value even for the standard interstellar grain-size distribution is subject to debate (Beckwith & Sargent 1993; see the review chapter by Beckwith); grain size evolution only complicates the picture (Miyake & Nakagawa 1993).

As noted in §3.2, micron-sized grains take times comparable to the age of disks to settle in quiescent nebulae. Any small grains left suspended in the disk after the bulk of the solid mass has sedimented to the midplane will remain suspended in the disk as long as it is quiescent. The effects of nebular turbulence on a suspended small grain population are harder to discern. By itself, turbulence causes small particles to remain stirred up and suspended in the nebula. However, turbulence also mixes these particles into the midplane region where they may collide and stick to larger bodies (Weidenschilling & Cuzzi 1993). The net result of these two competing processes on the small grain population is unknown. Also uncertain is how the turbulent properties change as the disk optical depth changes, *i.e.* whether the disk will remain turbulent as grain growth proceeds.

Current theoretical models cannot reliably predict how much of the initial solid mass will remain leftover as small particles, from processes such as particle shattering and erosion. The nebular models of Ruden & Lin (1986, Fig. 1) and Ruden & Pollack (1991) remain optically thick through mid-infrared wavelengths at all disk radii as long as  $\gtrsim 1\%$  of the initial grain mass remains suspended. The MMSN (Fig. 2) will also remain optically thick out to  $\lesssim 10$  AU under the same conditions. Finding observable signatures may require waiting until the disk gas is cleared (probably taking with it the small grain population) or searching for planet formation signatures in long wavelength regimes that remain optically thin.

### 3.5. FUTURE RESEARCH QUESTIONS

- What are the appropriate conditions in protostellar disks at the inception of the planet building epoch?
  - Do they resemble the MMSN?
  - Do different initial conditions lead to diverse planetary systems?
- What is the sticking probability in grain-grain collisions?
  - Do simulations using  $p_s = 1$  adequately model grain growth?
- Is planet formation inefficient?
  - How much solid mass is lost via gas-drag induced radial flow?
- How are planetesimals formed?
  - Via the Goldreich-Ward instability or by collisions?
- What are observable signatures of planet formation?

- Holes, or gaps, or warps?

#### 4. From Planetesimal to Planet

Planets are formed from the midplane planetesimal distribution by inelastic collisions. The key feature of the collisional evolution is that the cross-section for pairwise collisions can be increased above the geometrical value by gravitational attraction between the colliders (Safronov 1972). This result can be shown quite easily by considering energy and angular momentum conservation in the collision between two particles with masses  $m_1$  and  $m_2$  and radii  $a_1$  and  $a_2$ . In the center-of-mass system, the constant orbital energy and angular momentum are

$$E = \frac{1}{2}\mu v^2 - \frac{Gm_1m_2}{r} = \frac{1}{2}\mu V^2, \quad (19)$$

$$J = \mu |\mathbf{r} \times \mathbf{v}| = \mu r v \sin \theta = \mu b V, \quad (20)$$

where  $\mu = m_1m_2/(m_1 + m_2)$  is the reduced mass. In the rightmost equalities I have evaluated the constants  $E$  and  $J$  when the particles are at large separation where  $b$  is the impact parameter and  $V$  is the relative collision velocity. Without gravity the maximum impact parameter that results in a collision is the sum of the radii  $a_1 + a_2$ . With gravity, a grazing collision results when the minimum separation is  $r = a_1 + a_2$  and the velocity is purely tangential,  $\theta = \pi/2$ . Substituting these two conditions into equation (20) gives the speed at impact as  $v = bV/(a_1 + a_2)$ , which can be substituted into equation (19) to give the gravitationally enhanced cross-section for collision

$$\pi b^2 = \pi (a_1 + a_2)^2 \left[ 1 + \frac{v_e^2}{V^2} \right], \quad (21)$$

where the mutual escape speed,  $v_e$ , is

$$v_e = \sqrt{\frac{2G(m_1 + m_2)}{a_1 + a_2}}. \quad (22)$$

The term in brackets in equation (21) is the gravitational focusing factor and can greatly increase the cross-section above geometrical if the relative collision speed,  $V$ , is much smaller than the escape speed,  $v_e$ . Also note that if the focusing factor is large the cross-section is proportional to the fourth power of the particle radius (because  $v_e^2 \propto a^2$ ) rather than the second. In honor of Safronov's pioneering contributions to the study of collisional planet growth, the gravitational focusing factor is often written as  $1 + 2\theta$ , where  $\theta \equiv v_e^2/2V^2$ , is called the Safronov number. Detailed three-body

numerical orbit integrations confirm that the cross-section (21) is a good approximation (Ida & Nakazawa 1989; Greenzweig & Lissauer 1990, 1992).

The equation for the collisional growth of a planet with mass  $m_p = 4\pi\delta a^3/3$  (recall  $\delta$  is the internal density of the planet) accreting matter from a background “swarm” of planetesimals that move with respect to it at a relative speed  $V$  is (using the cross-section [21] and neglecting the size of the planetesimals)

$$\frac{dm_p}{dt} = \rho_s \cdot V \cdot \pi a^2 \left[ 1 + \frac{v_e^2}{V^2} \right], \quad (23)$$

where  $\rho_s$  is the volume density of the planetesimal swarm. We can rewrite this as an equation for the rate of change of the planetary radius

$$\frac{da}{dt} = \frac{1}{8} \left( \frac{\Omega \Sigma_s}{\delta} \right) \left[ 1 + \frac{v_e^2}{V^2} \right], \quad (24)$$

where  $\Sigma_s = 2\rho_s V/\Omega$  is the surface density of the planetesimal swarm (*c.f.* eq. [4]).

#### 4.1. ORDERLY GROWTH

The parameter that plays the most crucial role in determining the type of planetary growth is the Safronov number, *i.e.*, the magnitude of the planetary escape speed relative to the planetesimal velocity dispersion. Using a variety of analytical approaches, Safronov (1972) argued that as planetesimals accumulated, gravitational scattering off the largest member of the swarm would cause the velocity dispersion to keep pace with the escape speed from that member, regulating  $\theta$  to be near unity. In this scenario planets grow in an orderly fashion with most of the mass in the large bodies. From equation (24), the accumulation time is

$$\begin{aligned} t_{\text{orderly}} &= \frac{a}{da/dt} \approx \frac{1}{\Omega} \left( \frac{\delta a}{\Sigma_s} \right), \quad (\theta \sim 1) \\ &\approx 10^8 \left( \frac{r}{\text{AU}} \right)^3 \text{ years.} \end{aligned} \quad (25)$$

The growth time is determined by both the Kepler clock and the solid surface density. In the last line I have evaluated the growth time for Earth-sized bodies and taken  $\Sigma_s$  from the MMSN distribution (Fig. 2). These timescales are quite long, far greater than the lifetime of nebular disks, with the orderly growth process being unable to produce the cores of the outer giant planets in less than the age of the universe!

## 4.2. RUNAWAY GROWTH

The key to forming planets more rapidly is keeping the velocity dispersion small enough so that the gravitational focusing factor becomes very large ( $\theta \gg 1$ ). In this case, the most massive planetesimal in the swarm will have the largest collisional cross section ( $\propto a^4$ ), will grow more rapidly than any other body and will separate itself from the remainder of the swarm. Numerical models by Greenberg, *et al.* (1978) were the first to find this “runaway” path to planetary growth; subsequent calculations have confirmed these models (Wetherill & Stewart 1989, 1993; Ohtsuki & Ida 1990; Aarseth, Lin, & Palmer 1993). The basic mechanism behind runaway growth was elucidated by Wetherill & Stewart (1989) & (1993) Planetesimal velocities are determined by a balance among 1) stirring by gravitational scattering, 2) stirring by inelastic collisions, 3) damping due to energy dissipation in inelastic collisions, 4) damping due to gas drag, and 5) energy transfer from large to small bodies via dynamical friction (Lissauer & Stewart 1993). The most critical factor is dynamical friction, which tends to lead to an equipartition of kinetic energy among the bodies (Binney & Tremaine 1987), with the largest bodies having the smallest random velocities and thus the largest cross-sections. Figure 6 illustrates the runaway process in which the largest body grows the fastest as long as the velocity dispersion remains low.

Runaway growth can proceed until all the available material within the “accretion zone” (sometimes called the “feeding zone”) of the planet is consumed (Wetherill 1980; Lissauer 1987, 1993). The accretion zone is an annulus over which the planet can exert its gravitational influence to perturb nearby planetesimals into crossing orbits. The most common measure of the gravitational range of a planet of mass  $m_p$  a distance  $r$  away from a primary body of mass  $M_*$  is the Hill sphere (or Roche lobe radius) defined to be

$$r_H = r \left( \frac{m_p}{3M_*} \right)^{1/3}. \quad (26)$$

The origin of the cube root mass dependence comes from finding the region over which the gravity of the planet,  $Gm_p/r_H^2$ , dominates the tidal force of the primary object,  $(GM_*/r^2)(r_H/r)$ . The radial size of the accretion zone has been estimated to be a numerical factor  $B \approx 4$  times larger than the Hill sphere of the planet (Lissauer 1993). If the planet accretes all the available solid mass (with surface density  $\Sigma_s$ ) in an accretion zone having width  $B r_H$  on either side, its final “isolation” mass will be

$$m_p = 2\pi r \cdot 2Br_H \cdot \Sigma_s = 4\pi Br^2 \Sigma_s \left( \frac{m_p}{3M_*} \right)^{1/3}$$

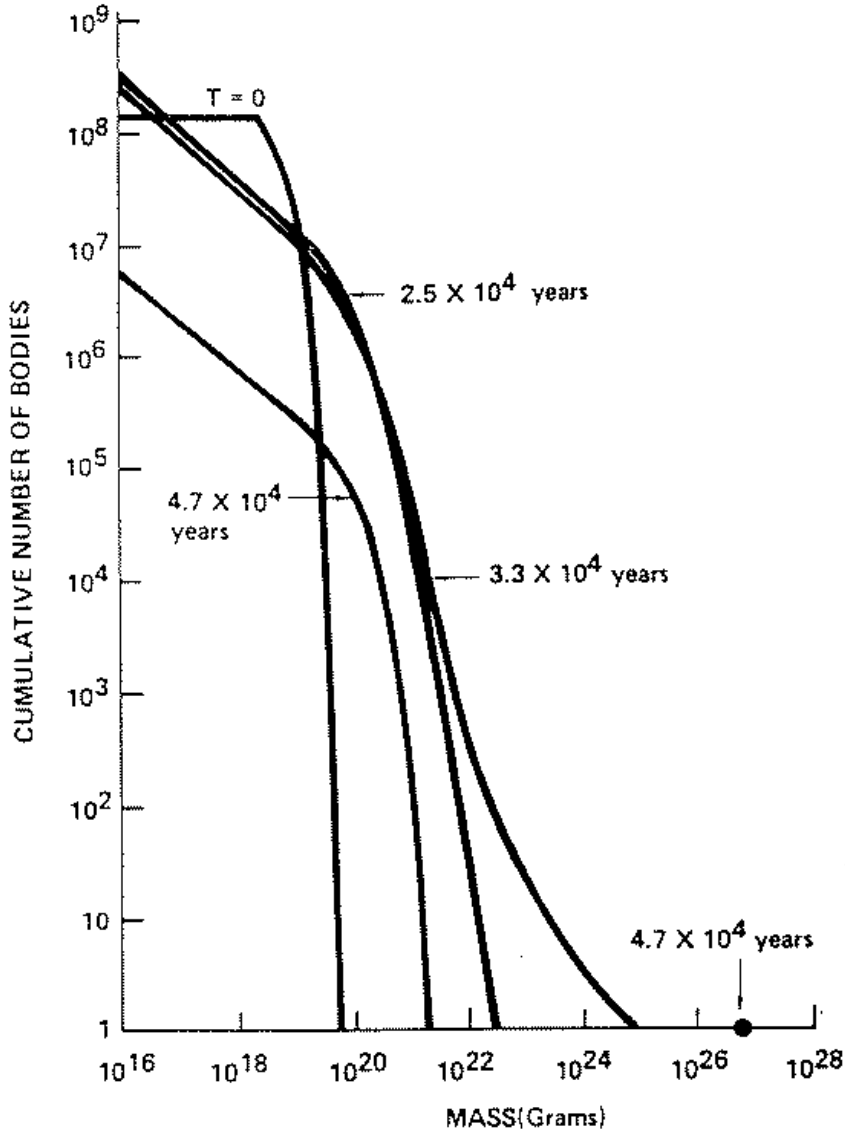
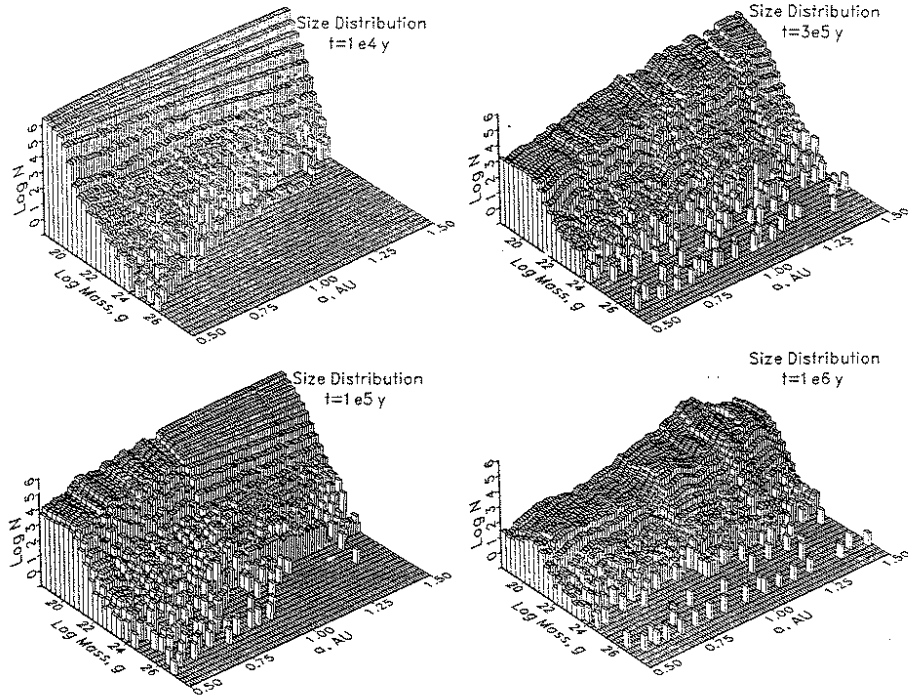


Figure 6. The evolution of the mass distribution of a planetesimal swarm between 0.99 and 1.01 AU illustrating the rapid runaway growth of the largest bodies. The most massive body becomes detached from the remainder of the swarm in less than  $5 \times 10^4$  years. See Wetherill & Stewart (1989).

$$= \frac{(4\pi B r^2 \Sigma_s)^{3/2}}{(3M_*)^{1/2}}. \quad (27)$$

The radial spacing of planets that have each become isolated is  $\approx 2Br_H$ . For the MMSN, we find an isolation mass of  $0.05M_\oplus$  at 1 AU and  $1.4M_\oplus$  at Jupiter's distance.



*Figure 7.* Accretional evolution of a planetesimal swarm near 1 AU. The number of planetesimals are plotted per logarithmic interval in mass as a function of distance from the Sun. The evolution is clearly more rapid at 0.5 AU than at 1.5 AU, but the final mass of the protoplanets ( $\sim 10^{27}$  g) is not dependent on distance from the Sun. Runaway growth is evident as the largest bodies separate themselves from the rest of the planetesimal population. After  $10^6$  years there are more bodies with lower mass than in the terrestrial region of the Solar System. From Weidenschilling, *et al.* (1997).

A recent detailed simulation of the accumulation of planetesimals in the terrestrial planet region has been performed by Weidenschilling, *et al.* (1997) that includes the processes mentioned above that control the velocity dispersion plus orbital perturbations caused by distant planetary bodies. The results of a simulation of the accumulation of  $2 M_\oplus$  of initially  $4.8 \times 10^{18}$  g (15 km) planetesimals spread between 0.5 and 1.5 AU is illustrated in Figure 7. These authors verified the critical role dynamical friction plays in producing rapid runaway growth. The first panel in Figure 7 ( $t = 10^4$  years) clearly shows the evolution to larger masses occurs

more rapidly at smaller radii where the Kepler frequency is larger. The other panels show that more massive bodies runaway and detach themselves from the distribution of lower mass planetesimals. Runaway growth produces bodies with masses  $\sim 10^{26}$  g in  $\lesssim 10^5$  years, but the growth rate slows as the velocity dispersion of the population of lower mass bodies increases, and the runaway stalls. By  $10^6$  years, about a dozen bodies with masses  $\approx 10^{27}$  g have been produced, but they are lower in mass and more closely spaced than the terrestrial planets. The masses (and separations) found in the simulation are about a factor of three larger than the analytic isolation mass in equation (27).

#### 4.3. FINAL ACCUMULATION STAGES

The outcome of runaway growth is self-limiting for two reasons. First, if the mass of the largest bodies becomes  $\sim 100$  times the median mass of the continuum bodies, the velocity dispersion of the lower mass planetesimals is pumped up by gravitational scattering, and the runaway slows (Ida & Makino 1993; Weidenschilling, *et al.* 1997). Second, even if the velocity dispersion remains small, all the mass within the accretion zone will be consumed by the planet, and it will become dynamically isolated with a mass given by equation (27). The evolution following runaway is much longer term as gravitational encounters slowly perturb the bodies into crossing orbits and violent impacts occur. The models described in §4.2, which start from MMSN-type conditions, do not yield masses and spacings similar to those of the terrestrial planets, hence, longer term collisional evolution is necessary to produce a final model that is similar to the Solar System. Figure 8 shows the results of six accumulation calculations by Wetherill (1988) that started with 500 bodies each of mass  $2 \times 10^{25}$  g. The outcome of each simulation is a small number of planets after about  $10^8$  years. The differences in the calculations illustrate the stochastic nature of the collisional accumulation. The long accumulation timescales do not present any serious difficulties for the terrestrial planets, which as noted in §1.1 could have completed their evolution in a gas-free environment. However the giant planet cores had to form in less than the lifetime of the gas disk, which seems to require a rapid runaway growth process occurring in a disk with solid mass larger than the MMSN (Lissauer 1987, 1993; eq. [27]).

#### 4.4. FUTURE RESEARCH QUESTIONS

- Can the Earth and the cores of giant planets be built directly from the runaway or is further long-term collisional growth needed?
  - How do you build the giant planet cores before the gas is dis-

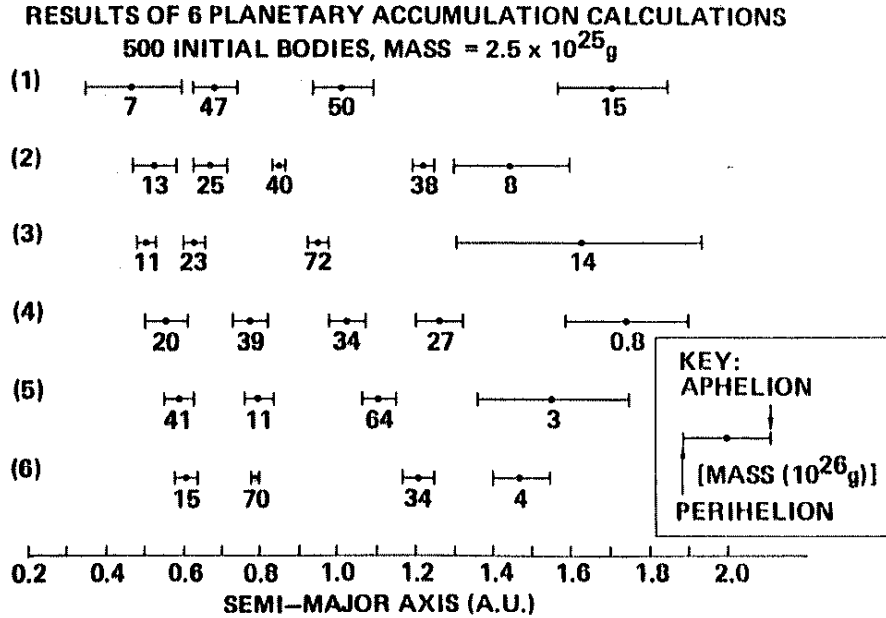


*Figure 8.* Six calculations of terrestrial planet accumulation by Wetherill (1988). The final mass of each planet in units of  $10^{26}$  g is indicated ( $1M_{\oplus} = 60$  in these units). The semimajor axis, with a bar extending from perihelion to aphelion, is also shown. From Lissauer (1993).

persed?

- How does the final planetary system depend on the initial disk mass distribution?
  - Do higher mass disks produce *more* planets or fewer, but higher-mass, planets?
- Can *rocky* planets with masses comparable to Jupiter be built in protoplanetary disks?

## 5. The Formation of Gas Giant Planets

### 5.1. THE CORE-INSTABILITY SCENARIO

The current model for the formation of gas giant planets is that they follow the path outlined above and begin as rocky cores. Mizuno (1980) showed that a gas envelope gravitationally bound to a rocky core cannot remain in hydrostatic equilibrium if the core mass exceeds a critical value  $\sim 10 - 15 M_{\oplus}$ , comparable to the core masses inferred for the giant

planets (Hubbard & Marley 1989; Chabrier, *et al.* 1992). Subsequent time-dependent calculations (Bodenheimer & Pollack 1986; Pollack, *et al.* 1996; see top panel in Fig. 9) have shown the nebular gas is rapidly accreted by the rocky core once its mass is above critical, leading to the conversion of a rocky planet into a gas giant planet. Before the critical core mass is reached, the radiated luminosity of the planet is supplied primarily by the gravitational energy of the accreted planetesimals. As the gravitationally bound gas envelope becomes more massive, planetesimal accretion is unable to supply the luminosity needed to maintain the extended envelope and rapid (but not hydrodynamic) collapse of the envelope takes place, with the gravitational contraction of the envelope supplying the luminosity. As the envelope contracts, surrounding nebular gas flows in, and the gas accretion rate rises to become orders of magnitude larger than the solid accretion rate. The evolutionary timescale shortens; the gas envelope of Jupiter is accreted in  $\lesssim 10^5$  years (Pollack, *et al.* 1996). Detailed calculations show the value of the critical core mass ( $\sim 10 - 30 M_{\oplus}$ ) is only moderately dependent on orbital radius and nebular properties and depends most strongly on the planetesimal accretion rate (see Stevenson [1982] for a simple analytical calculation of the critical core mass).

In the core-instability model, giant planets are composite bodies with the rocky cores forming first and the gas envelopes accreting afterwards. If this model is correct, there is a logical simplicity to the formation of planetary systems - all planets are born by the accumulation of solids; giant planets are higher mass cores that happen to accrete large gas envelopes. The core-instability model is not without problems, however. First, it is not obvious that  $\gtrsim 10M_{\oplus}$  solid cores can form before the nebular gas is dispersed. Runaway growth to the critical mass requires solid densities about four times larger than in the MMSN (see eq. [27]). Forming the cores in  $\sim 10^6$  years requires a large net gravitational focusing factor ( $\theta \gtrsim 10^3$ ), which requires a very cold population of accreting planetesimals. Even if such cores can be formed at the orbit of Jupiter, it is not clear they can be formed so quickly at the orbits of Uranus or Neptune where the Kepler clock runs more slowly. Second, this model does not explain what *halts* the accretion of gas onto the planets. While it is possible the nebular gas was dispersed rapidly during the giant planet gas accretion phase, severe timing constraints (dispersal in  $\lesssim 10^5$  years) make this unlikely. The most plausible explanation is that planetary gravitational tides become strong enough to “repel” nearby gas once the planet is sufficiently massive (Lin & Papaloizou 1993; see the next section). Finally, it is not clear from the internal structure of the giant planets in our Solar System that all four actually went critical. The large gas masses of Jupiter and Saturn seem to require their cores to have reached critical mass, but the smaller envelope

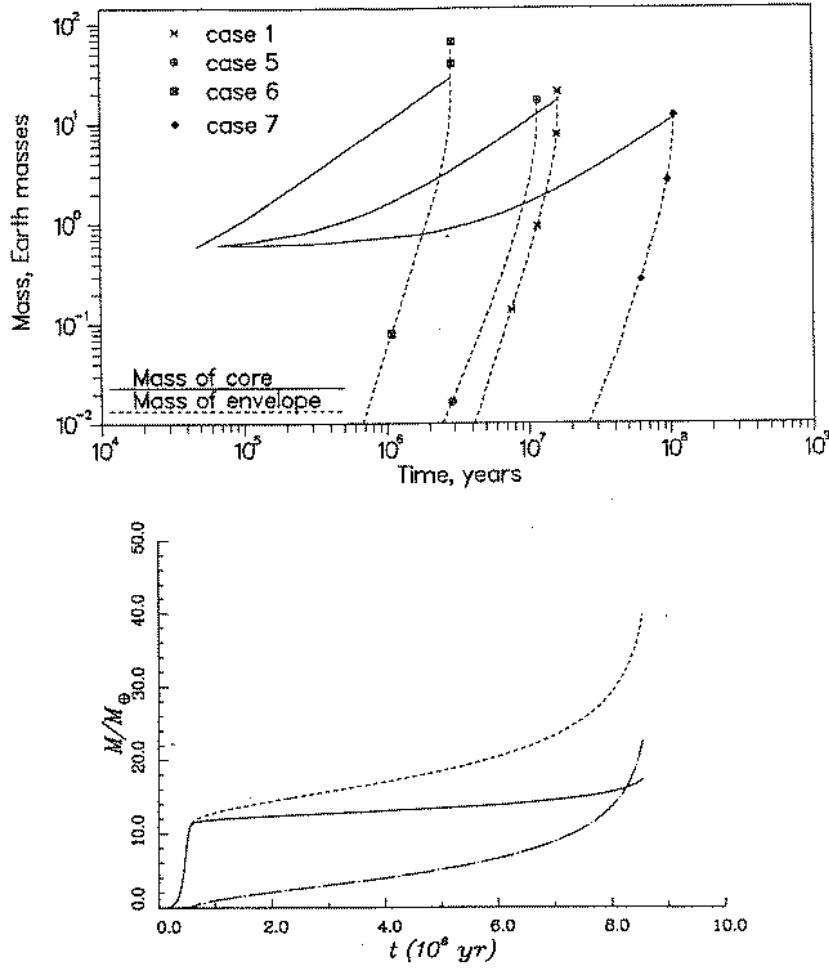


*Figure 9.* Core-Instability Model. **Top panel** from Bodenheimer & Pollack (1986) shows the core mass (solid) and envelope mass (dotted) as a function of time. Cases 6, 1 & 5, and 7 have constant planetesimal accretion rates of  $10^{-5}$ ,  $10^{-6}$ , and  $10^{-7}$   $M_{\oplus}/\text{yr}$ , respectively. Case 5 has grain opacity reduced by 50 to reflect the decreased dust-to-gas ratio after solids have sedimented from the gas. The envelope mass is very small until the critical core mass is reached (defined to occur when  $M_{\text{core}} = M_{\text{env}}$ ). At that point rapid gas accretion ensues. **Bottom panel** from Pollack, *et al.* (1996) shows the core mass (solid), envelope mass (dot-dashed) and total mass (dotted) as a function of time. Rather than assuming constant planetesimal accretion rates (as in the top panel), this calculation uses more detailed and self-consistent planetesimal accretion rates. The initial core forms by runaway in less than  $10^6$  years after which the growth rate slows. The planet becomes critical after  $\approx 8 \times 10^6$  years, when rapid gas accretion begins.

masses of Uranus and Neptune ( $M_{\text{env}} \lesssim 0.5 M_{\text{core}}$ ) imply these planets did not. Shu, Johnstone, & Hollenbach (1993) have discussed how photoevapo-

ration of the disk by the ultraviolet flux from the central star preferentially removes disk gas beyond  $\sim 10$  AU (the orbital distance of Saturn), which may explain the smaller gas mass reservoir available for the outer planets. Recent calculations of the core-instability model that adopt more realistic planetesimal accretion rates (Pollack, *et al.* 1996) indicate the planets experience a long phase ( $\sim 7 \times 10^6$  year) after core runaway in which the envelope mass is smaller than the core mass (see bottom panel in Fig. 9). If the nebula were removed during this long phase of “stalled” gas accretion, the resulting planets would be similar to the outer giants.

## 5.2. TIDAL INTERACTION

Gravitational interactions between orbiting mass points and disks has been considered by many authors (Goldreich & Tremaine 1979; Lin & Papaloizou 1979; Ward & Hourigan 1989; Takeuchi, Miyama, & Lin 1996; see review by Lin & Papaloizou 1993). The essential physics can be elucidated by using the impulse approximation (Lin & Papaloizou 1979). As gas flows by the planet interior (exterior) to its orbital radius, the planet’s gravitational field causes a slight deflection in the gas streamlines causing the angular momentum of the gas to decrease (increase). The gravitational tidal interaction allows angular momentum to be transferred from the gas on the inside to the planet and from the planet to the gas on the outside. Because orbital angular momentum increases outward in dynamically stable disks (the Rayleigh criterion; Drazin & Reid 1981), gas interior (exterior) to the planet that loses (gains) angular momentum in the tidal exchange must move farther inward (outward). In effect, the gravitational tides of the planet act to *repel* nearby gas. In a fluid dynamical context (Goldreich & Tremaine 1979), the tides of the planet excite spiral density waves that propagate away from the planet (in the absence of disk self-gravity). The waves are excited at Lindblad resonances, locations in the disk where the natural frequency of radial oscillation (the epicyclic frequency) is an integer multiple of the frequency at which the gas is forced by the planet.<sup>5</sup> Spiral density waves carry angular momentum, which is deposited in the gas as the waves are damped by viscous stresses. Figure 10 illustrates the situation schematically. The total torque on the gas is found by summing the contributions from all the Lindblad resonances; it is negative (positive) for the gas interior (exterior) to the planet. The magnitude of the torque at either the

<sup>5</sup>For Kepler disks, the Lindblad resonances are at radii satisfying  $\pm m(\Omega(r) - \Omega_p) = \Omega(r)$ , where  $\Omega_p$  is the orbital frequency of the planet and  $m$  is a positive integer. The positive (negative) sign is for inner (outer) resonances.

inner or outer resonances,  $T_{\text{tidal}}$ , is approximately (Lin & Papaloizou 1993)

$$T_{\text{tidal}} \approx f \Sigma \Omega_p^2 r_p^4 \left( \frac{r_p}{H} \right)^3 \left( \frac{m_p}{M_*} \right)^2, \quad (28)$$

where  $\Omega_p$  is the rotation frequency evaluated at the planetary radius  $r_p$ ,  $H$  is the vertical height of the disk and  $f \approx 0.2$  is a numerical constant. This torque is deposited in the vicinity of the planet unless the viscosity is too small to damp the waves locally. The *net* tidal torque, which is the sum of the two nearly equal and opposite inner and outer contributions, is difficult to calculate precisely but is roughly a factor  $H/r$  smaller than (28) (Ward 1986).

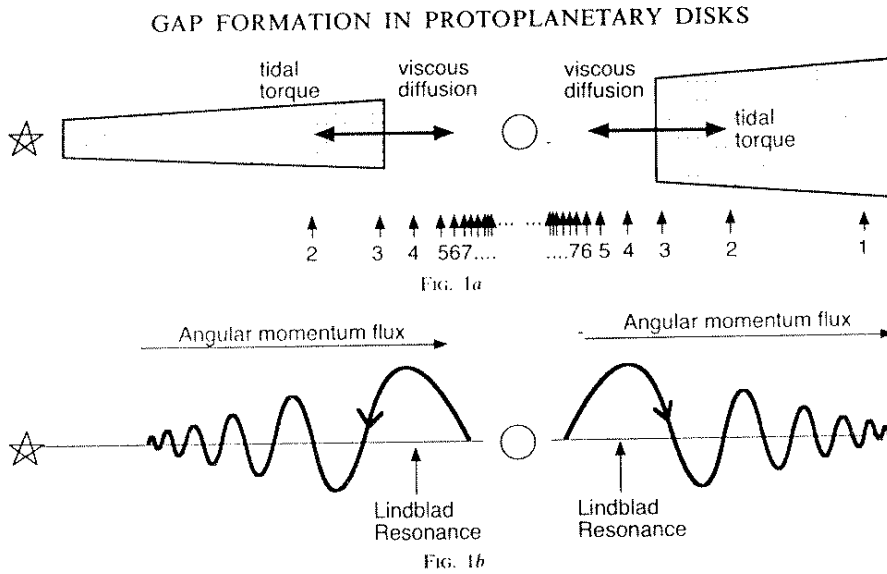


*Figure 10.* Formation of gaps in disks from Takeuchi, Miyama, & Lin (1996). **Top Panel.** Schematic illustration shows that gaps are formed from a balance between tidal torques that repel gas from the planet and viscous stresses that diffuse gas back into the gap. The tidal torque is actually deposited at the Lindblad resonances (indicated by arrows). **Bottom Panel.** Schematic illustration of wave propagation in disks. Waves are excited at the inner and outer Lindblad resonances and propagate away from the planet. As they damp, the angular momentum they carry is deposited into the gas as a tidal torque. A net outward flux of angular momentum results.

The action of the planetary tidal torques, which tend to push gas away from the planet, is opposed by the viscous stress of the gas, which tends to diffuse gas back toward the planet. The viscous torque on the disk gas,  $T_{\text{vis}}$ , is (Lynden-Bell & Pringle 1974)

$$T_{\text{vis}} = 3\pi \Sigma \nu \Omega r^2 = 3\pi \alpha \Sigma \Omega^2 r^4 \left( \frac{H}{r} \right)^2, \quad (29)$$

using equations (3) and (7) to get the rightmost form. The criterion for the planet to open an annular gap at its orbital radius is that the gravitational tidal torque exceed the viscous torque,  $T_{\text{tidal}} \gtrsim T_{\text{vis}}$ . Using equations (28) and (29) the minimum planet mass,  $m_{\text{p}}$ , needed to open a gap is (Takeuchi, Miyama, & Lin 1996)

$$\frac{m_{\text{p}}}{M_*} \gtrsim \sqrt{\frac{3\pi}{f}} \left(\frac{H}{r}\right)^{5/2} \alpha^{1/2}. \quad (30)$$

For typical solar nebular parameters this gives a mass of  $\sim 75M_{\oplus}$ , slightly less than the mass of Saturn. It thus seems reasonable that Jupiter and Saturn (but not Uranus or Neptune unless the disk was extremely cold) were able to form gaps in the surface density distribution, reducing the local gas density to small values and possibly terminating the rapid gas accretion phase. I note however that some recent hydrodynamical simulations of the gap formation process though have questioned whether gap formation completely halts gas accretion onto the planet. The simulations indicate that even if a low density gap is formed, the planet remains connected to the gap walls by arc-like streams through which gas can flow (Artymowicz & Lubow 1996, personal communication 1998). Clearly far more work is needed to determine whether the formation of a gap completely halts gas accretion, and if not, what determines the final mass of the giant planets.

### 5.3. TIDAL MIGRATION

An essential consequence of the tidal exchange of angular momentum between the planet and disk is that a net torque can act on the planet, causing its orbital radius to change with time. This process is known as orbital or tidal *migration* (Lin & Papaloizou 1986; Ward 1997). The angular momentum of the planet (on a circular orbit) is  $m_{\text{p}}\Omega_{\text{p}}r_{\text{p}}^2 = m_{\text{p}}(GM_*r_{\text{p}})^{1/2}$  and writing the *net* tidal torque exerted by the planet on the gas disk as  $T_{\text{net}}$ , the orbital evolution of the planet is governed by

$$\frac{d}{dt} (m_{\text{p}}\Omega_{\text{p}}r_{\text{p}}^2) = -T_{\text{net}}, \quad (31)$$

or equivalently

$$\frac{dr_{\text{p}}}{dt} = -\frac{2}{m_{\text{p}}\Omega_{\text{p}}r_{\text{p}}} T_{\text{net}}. \quad (32)$$

The orbital migration timescale is

$$\begin{aligned} t_{\text{mig}} &= \frac{r_{\text{p}}}{|dr_{\text{p}}/dt|} = \frac{\Omega_{\text{p}}r_{\text{p}}^2}{2T_{\text{net}}}, \\ &\sim \frac{1}{\Omega_{\text{p}}} \left(\frac{M_*}{m_{\text{p}}}\right) \left(\frac{M_*}{\Sigma r_{\text{p}}^2}\right) \left(\frac{H}{r}\right)^2, \quad (\text{no gap}) \end{aligned} \quad (33)$$

where I have used equation (28) reduced by  $H/r$  to estimate the net torque (Ward 1986). This equation is appropriate for lower mass planets that do not tidally truncate the disk and form gaps. For planets massive enough to form gaps, the surface density in their vicinity is reduced dramatically, and equation (33) does not apply. Numerical calculations of the combined gap formation and tidal migration process (Lin & Papaloizou 1993) show that the inner and outer torques nearly cancel and the evolution time becomes the *local* viscous diffusion time, equation (8), applied at the orbit of the planet. Figure 11 illustrates a self-consistent calculation of gap formation and tidal migration in a protoplanetary disk.

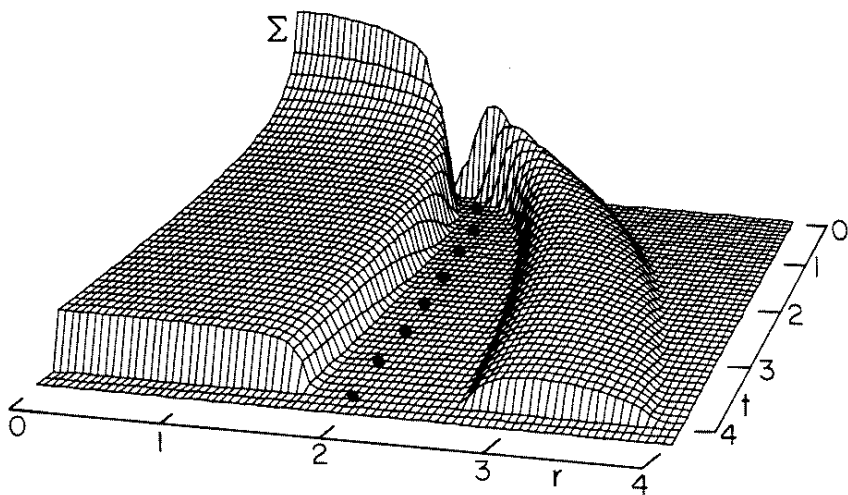


*Figure 11.* Tidal migration of a protoplanet in an evolving nebula from Lin & Papaloizou (1993). Surface density,  $\Sigma$ , is plotted versus distance from star,  $r$ , as a function of time,  $t$ . All variables are scaled and dimensionless. Notice the surface density decreases with time (due to accretion), and the outer disk radius increases. The position of the planet is marked by a dot. The mass of the planet is large enough that tides overcome viscous stresses, and a gap forms near the planet (the region where  $\Sigma \rightarrow 0$ ). In this example, the planet is near the outer disk radius and migrates outward as it absorbs angular momentum from the inner disk. Eventually the inner disk will be accreted by the star, and the planet will migrate inward. The migration timescale is the viscous timescale of the disk.

The tidal migration timescale is surprisingly short. Using values appropriate to the MMSN, the timescale (33), appropriate for planets not forming gaps, is  $t_{\text{mig}} \approx (M_*/m_p)(r/\text{AU})$  years, which is about  $3 \times 10^5$  years for the Earth. For planets massive enough to form gaps, the ratio of the viscous time at their orbital distance to the overall viscous time of the disk (having outer radius  $R_D$ ) is  $\sim (r_p/R_D)^{3/2}$ , from equation (8) assuming  $H/r$

is roughly constant. Because Jupiter and Saturn were well within the outer radius of the primordial solar nebula ( $r_p \ll R_D$ ), their migration times were much shorter than the  $\sim 10^7$  year lifetime of the disk as a whole. Figure 12 shows a calculation of the orbital migration of Jupiter and Saturn in which a migration time of  $\sim 10^5$  years is found.

#### 5.4. THE SURVIVAL OF GIANT PLANETS

Tidal migration offers a neat way to explain the recently discovered Jupiter-mass planets having orbital distances of  $\lesssim 0.1$  AU from their stars (Marcy & Butler 1998; also see the review by Marcy in this volume) if a mechanism can be found to *halt* the migration before the planets are swallowed by the star. The key is to find an outward torque that can counterbalance the inward tidal torque. Lin, Bodenheimer & Richardson (1996) have suggested that as the planet nears the central star, it will raise tidal bulges in the star that will transfer angular momentum from the spin of the star to the planetary orbit. This spin-orbit coupling can be effective at keeping the planet beyond the corotation radius (the distance in the disk where the Kepler orbital frequency equals the stellar rotation frequency). These authors also suggest that a star with a sufficiently strong magnetic field will have a magnetosphere that truncates the disk at a distance of several stellar radii. Once the planet migrates inside the inner disk edge, the inward tidal torques vanish because the surface density is negligible. Either mechanism can produce planets in orbits near the star.

Trilling, *et al.* (1998) have considered a mechanism involving mass loss from the planet. The size of the planetary Roche lobe (*c.f.* eq. [26]) is proportional to the distance from the star. As a giant planet migrates inward, it can fill its Roche lobe, leading to a transfer of mass from the planet to the star. Conservation of angular momentum of the system requires the planet to move outward. Stable mass transfer is achieved when the planet orbits at a distance where its radius equals its Roche radius. Planets in small orbits near stars can be produced if the disk is dissipated before the planet loses all its mass.

Our own Solar System with planets distributed from 0.4 - 30 AU does not show signs of appreciable orbital migration, however. The question in our Solar System is to understand how the large orbital migrations apparently observed in other planetary systems were avoided. Because the migration timescale becomes the viscous timescale for planets massive enough to form gaps, a giant planet can avoid appreciable migration if it is born in a low viscosity nebula having evolutionary times comparable to or longer than the disk dispersal time. Before the planet has time to migrate far, the nebular gas is dispersed, and the migration is halted. Denoting the disk

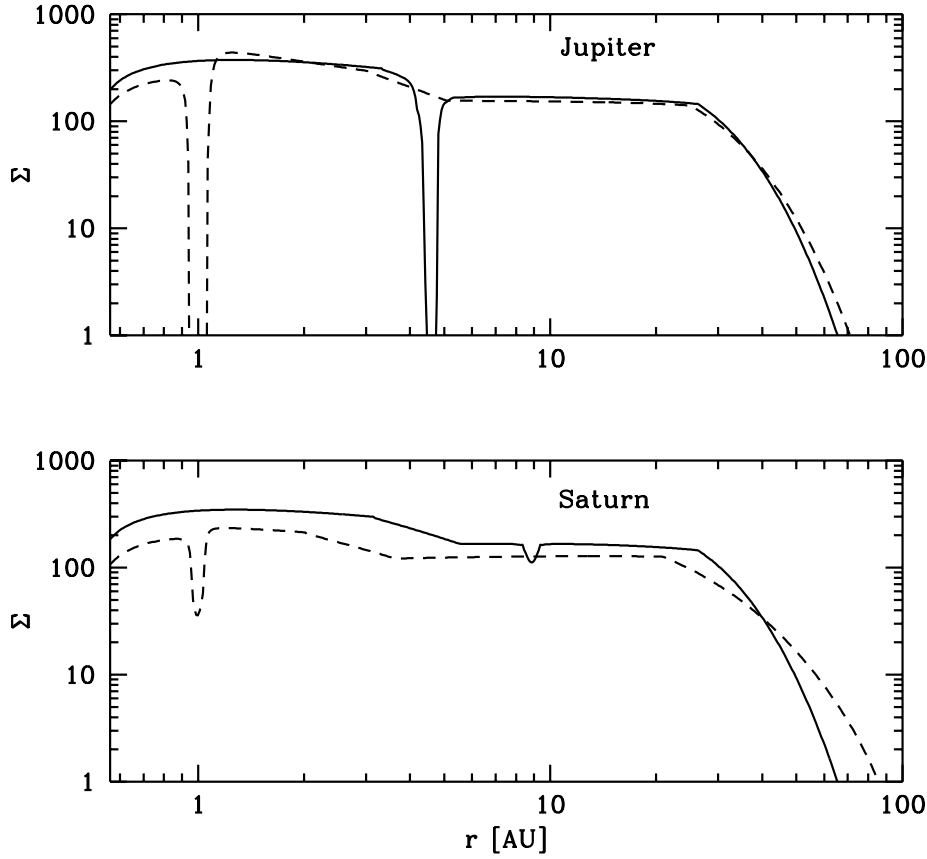


*Figure 12.* Tidal migration in the solar nebula models of Ruden & Lin (1986). Surface density in  $\text{g/cm}^2$  is plotted versus distance from the Sun in AU. Jupiter is assumed to form instantaneously with its present mass and orbital radius at a time in the nebular evolution when it is just massive enough to form a gap (eq. [30]). Saturn is assumed to form coevally. **Top panel.** The solid curve is  $10^3$  years after Jupiter formation showing the gap (the region where  $\Sigma$  drops to zero) is formed rapidly. The dashed curve is  $4 \times 10^4$  years later, showing Jupiter has migrated inward to 1 AU. **Bottom panel.** The solid curve is also  $10^3$  years after Saturn formation. Saturn does not form a gap, but the surface density is reduced there by 30%. The dashed curve is  $1.5 \times 10^5$  years later. At this later time, the surface density in the gap is not zero but has been reduced by a factor of 5. The average inward migration speeds are about 40 cm/s for either planet.

dispersal time by  $t_{\text{disp}}$ , we can estimate from equation (8) that this requires the viscous alpha parameter to be  $\lesssim (r/H)^2 / (\Omega t_{\text{disp}})$ . Using  $r/H \approx 25$  and  $t_{\text{disp}} \sim 10^7$  years, I find  $\alpha \lesssim 10^{-4}$  is sufficiently small that migration of Jupiter will not be severe. It is not unreasonable that giant planets form in

a low viscosity environment. The lower panel in Figure 9 shows a model for the formation of Jupiter in which rapid gas accretion does not begin until  $t \sim 8 \times 10^6$  years. In this model, the newly formed Jupiter would find itself in a nebular environment that had undergone significant evolution. The disk mass at that epoch could be quite small, with the corresponding low surface densities leading to small tidal torques and low migration rates. In fact, given that the MMSN contains only 10 – 20 Jupiter masses, formation of the giant planets at a late epoch when the gas mass may be appreciably less than in the MMSN may require the giant planets to accrete a large fraction of the remaining disk mass.

### 5.5. FUTURE RESEARCH QUESTIONS

- Is the core-instability model the only way to make giant planets?
  - Did the dispersal of the disk prevent Uranus and Neptune from going critical?
- What determines the final masses and orbital distances of the giant planets?
  - Does gap formation halt gas accretion onto giant planets?
  - What prevented significant orbital migration from occurring in our Solar System?
- How does the planetary mass spectrum merge into the brown dwarf mass spectrum?
  - Do brown dwarfs form in a fundamentally different manner than planets, *e.g.*, from collapse/fragmentation of the disk rather than from accumulation of dust?

### *Acknowledgments*

I would like to thank Charlie Lada and Nick Kylafis for inviting me to the beautiful island of Crete for the second Star Formation summer school. This work has been supported in part by NSF AST-9157420 and NASA NAGW-5122.

### References

- Aarseth, S. J., Lin, D. N. C., Palmer, P. L. 1993, ApJ, 403, 351  
 Adachi, I., Hayashi, C., Nakagawa, K. 1976, Prog Theor Phys, 56, 1756  
 Adams, F. C., Lada, C. J., Shu, F. H. 1987, ApJ, 312, 788  
 Adams, F. C., Lin, D. N. C. 1993, in *Protostars & Planets III*, eds. E. H. Levy & J. I. Lunine, (Tucson: University of Arizona Press), 721  
 Artymowicz, P., Lubow, S. H. 1996, ApJ Lett, 467, L77  
 Balbus, S. A., Hawley, J. F. 1991, ApJ, 376, 214  
 Beckwith, S. V. W., Sargent, A. I. 1993, in *Protostars & Planets III*, eds. E. H. Levy & J. I. Lunine, (Tucson: University of Arizona Press), 521

- Beckwith, S., Sargent, A. 1996, *Nature*, 383, 139
- Beckwith, S. V. W., Sargent, A. I., Chini, R. S., Gusten, R. 1990, *AJ*, 99, 924
- Binney, J., Tremaine, S. D. 1987, *Galactic Dynamics*, (Princeton: Princeton University Press)
- Blum, J., Münch, M. 1993, *Icarus*, 106, 151
- Bodenheimer, P., Pollack, J. B. 1986, *Icarus*, 67, 391
- Bridges, F. G., Supulver, K. D., Lin, D. N. C., Knight, R., Zafra, M. 1996, *Icarus*, 123, 422
- Brown, H. 1949, in *The Atmospheres of the Earth and Planets*, ed. G. P. Kuiper, (Chicago: Univ. of Chicago Press), 258
- Butler, R. P., Marcy, G. W. 1996, *ApJ Lett*, 464, L153
- Cameron, A. G. W. 1978, in *Protostars and Planets*, ed. T. Gehrels, (Tucson: Univ. of Arizona Press), 453
- Chabrier, G., Saumon, D., Hubbarb, W. B., Lunine, J. I. 1992, *ApJ*, 391, 817
- Chambers, J. G., Wetherill, G., Boss, A. 1996, *Icarus*, 119, 261
- Cuzzi, J. N., Dobrovolskis, A. R., Champney, J. M. 1993, *Icarus*, 106, 102
- Drazin, P. G., Reid, W. H. 1981, *Hydrodynamic Stability*, (Cambridge: Cambridge University Press), pp. 69
- Dubrulle, B. 1993, *Icarus*, 106, 59
- Goldreich, P., Tremaine, S. 1979, *ApJ*, 233, 857
- Goldreich, P., Ward, W. R. 1973, *ApJ*, 183, 1051
- Greenberg, R., Wacker, J. F., Hartmann, W. L., Chapman, C. R. 1978, *Icarus*, 35, 1
- Greenzweig, Y., Lissauer, J. J. 1990, *Icarus*, 87, 40
- Greenzweig, Y., Lissauer, J. J. 1992, *Icarus*, 100, 440
- Hartmann, L., MacGregor, K. B. 1982, *ApJ*, 259, 180
- Hayashi, C. 1981, *Prog Theor Phys Supp*, 70, 35
- Hubbard, W. B., Marley, M. S. 1989, *Icarus*, 78, 102
- Ida, S., Makino, J. 1993, *Icarus*, 106, 210
- Ida, S., Nakazawa, K. 1989, *Astron Ap*, 224, 303
- Koerner, D. W., Ressler, M. E., Werner, M. W., Backman, D. E. 1998, *ApJ Lett*, 503, L38
- Lin, D. N. C., Bodenheimer, P., Richardson, D. C. 1996, *Nature*, 380, 606
- Lin, D. N. C., Papaloizou, J. C. B. 1979, *MNRAS*, 186, 789
- Lin, D. N. C., Papaloizou, J. C. B. 1980, *MNRAS*, 191, 37
- Lin, D. N. C., Papaloizou, J. 1985, in *Protostars and Planets II*, eds. D. C. Black & M. S. Matthews, (Tucson: Univ. of Arizona Press), 981
- Lin, D. N. C., Papaloizou, J. 1986, *ApJ*, 309, 846
- Lin, D. N. C., Papaloizou, J. C. B. 1993, in *Protostars and Planets III*, eds. E. H. Levy & J. I. Lunine, (Tucson: Univ. of Arizona Press), 749
- Lin, D. N. C., Pringle, J. E. 1987, *MNRAS*, 358, 515
- Lissauer, J. J. 1987, *Icarus*, 69, 249
- Lissauer, J. J. 1993, *Ann. Rev. Astron. Ap.*, 31, 129
- Lissauer, J. J., Stewart, G. R. 1993, in *Protostars and Planets III*, eds. E. H. Levy & J. I. Lunine, (Tucson: Univ. of Arizona Press), 1061
- Lynden-Bell, D., Pringle, J. E. 1974, *MNRAS*, 168, 603
- Marcy, G. W., Butler, R. P. 1996, *ApJ Lett*, 464, L147
- Marcy, G. W., Butler, R. P. 1998, *Ann. Rev. Astron. Ap.*, 36, 57
- Markiewicz, W. J., Mizuno, H., Völk, H. J. 1991, *Astron Ap*, 242, 286
- Mayor, M., Queloz, D. 1995, *Nature*, 378, 355
- Miyake, K., Nakagawa, Y. 1993, *Icarus*, 106, 20
- Mizuno, H. 1980, *Prog Theor Phys*, 96, 266
- Mizuno, H. 1989, *Icarus*, 80, 189
- Nakagawa, Y., Hayashi, C. 1981, *Icarus*, 45, 517
- Nakagawa, Y., Nakazawa, K., Hayashi, C. 1981, *Icarus*, 45, 517
- Ohtsuki, K., Ida, S. 1990, *Icarus*, 85, 499

- Pepin, R. O. 1989, in *Origin and Evolution of Planetary and Satellite Atmospheres*, eds. S. K. Atreya, J. B. Pollack, M. S. Matthews, (Tucson: University of Arizona Press), 291
- Pollack, J. B., Hubickyj, O., Bodenheimer, P., Lissauer, J. J., Podolak, M., Greenzweig, Y. 1996, *Icarus*, 124, 62
- Pringle, J. E. 1981, *Ann Rev Astron Ap*, 19, 137
- Prinn, R. G. 1982, *Planet Sp Sci*, 30, 741
- Ruden, S. P. 1998, in preparation
- Ruden, S. P., Lin, D. N. C. 1986, *ApJ*, 308, 883
- Ruden, S. P., Pollack, J. B. 1991, *ApJ*, 375, 740
- Safronov, V. S. 1972, *Evolution of the Protoplanetary Cloud and Formation of the Earth and Planets*, NASA TT-F-677
- Shakura, N. J., & Sunyaev, R. A. 1973, *Astron Ap*, 24, 337
- Shu, F. H., Adams, F. C., Lizano, S. 1987, *Ann. Rev. Astron. Ap.*, 25, 23
- Shu, F. H., Johnstone, D., Hollenbach, D. 1993, *Icarus*, 106, 92
- Shu, F. H., Tremaine, S., Adams, F. C., Ruden, S. P. 1990, *ApJ*, 358, 495
- Stepinski, T. F., Levy, E. H. 1990, *ApJ*, 350, 819
- Stevenson, D. J. 1982, *Planet Sp Sci*, 30, 755
- Strom, S. E., Strom, K. M., Edwards, S., Cabrit, S., Skrutskie, M. F. 1989, *AJ*, 97, 1451
- Supulver, K. D., Bridges, F. D., Tiscareno, S., Lievore, J., Lin, D. N. C. 1997, *Icarus*, 129, 539
- Takeuchi, T., Miyama, S. M., Lin, D. N. C. 1996, *ApJ*, 460, 832
- Trilling, D., Benz, W., Guillot, T., Lunine, J. I., Hubbard, W. B., Burrows, A. 1998, *ApJ*, 500, 428
- Ward, W. R. 1986, *Icarus*, 67, 164
- Ward, W. R. 1997, *Icarus*, 126, 261
- Ward, W. R., Hourigan, K. 1989, *Icarus*, 347, 490
- Wardle, M., Königl, A. 1993, *ApJ*, 410, 218
- Weidenschilling, S. J. 1977a, *Astrophys Sp Sci*, 51, 153
- Weidenschilling, S. J. 1977b, *MNRAS*, 180, 57
- Weidenschilling, S. J. 1984, *Icarus*, 60, 553
- Weidenschilling, S. J., Cuzzi, J. N. 1993, in *Protostars and Planets III*, eds. E. H. Levy & J. I. Lunine, (Tucson: Univ. of Arizona Press), 1031
- Weidenschilling, S. J., Spaute, D., Davis, D. R., Marzari, F., Ohtsuki, K. 1997, *Icarus*, 128, 429
- Wetherill, G. W. 1988, in *Mercury*, eds. C. Chapman, F. Vilas, (Tucson: University of Arizona Press), 670
- Wetherill, G. W. 1990, *Ann Rev Earth Plan Sci*, 18, 205
- Wetherill, G. W., Stewart, G. R. 1989, *Icarus*, 77, 330
- Wetherill, G. W., Stewart, G. R. 1993, *Icarus*, 106, 190
- Whipple, F. L. 1972, in *From Plasma to Planets*, ed. A. Elvius, (New York: Wiley), 211
- Wurm, G., Blum, J. 1998, *Icarus*, 132, 125
- Zuckerman, B., Forveille, E., Kastner, J. H. 1995, *Nature*, 373, 494